Particle delivery in optical conveyor belt: optimal delivery speed and the influence of viscosity near surface

Martin Šiler, Tomáš Čižmár, Mojmír Šerý, Petr Jákl and Pavel Zemánek

Institute of Scientific Instruments, Academy of Sciences of the Czech Republic,
Královopolská 147, 612 64 Brno, Czech Republic

Abstract

Travelling standing wave (TSW) sometimes called optical conveyor belt (OCB) can be used to deliver Brownian particles in one dimension in a controlled way. Thermal noise causes that the speed of the particle delivery is not generally the same as the speed of the TSW because the particle hops between neighboring stable equilibrium positions (optical traps). These hops slow down the speed of the particle delivery and two limiting cases can be distinguished. *Brownian surfer* is obtained if the standing wave travels slowly and provides potential wells deep enough so that the particle is tightly coupled to the well and "surfs along with the potential wave". If the velocity of the TSW is high and the potential well is shallower, the particle - *Brownian swimmer* is not dragged by the wave in motion and behaves more like a swimmer afloat on the surface of the ocean.

Conclusions

- The average bead velocity was derived theoretically by means of Fokker-Planck equation. The conditions for "surfer" and "swimmer" cases were discussed.
- The behavior of bead in motional standing wave was studied by Monte-Carlo simulations in one dimension. The simulations validated theoretical predictions.
- Evanescent wave conveyor belt was used to compare theoretical results with experiment.
- We found that the separation of bead from the interface varies during the motion of standing wave. Assuming constant "mean bead–surface separation" we have been able to obtain a good coincidence between observed mean particle velocity and its theoretical prediction.

Illustration of surfer and swimmer cases

We assume that a microbead is located in a periodic array of optical traps travelling with constant velocity v. An interference of two counterpropagating plane waves creates a potential profile $U(x) = \Delta U/2\cos(4\pi n_{\text{ext}}x/\lambda)$, where ΔU is the potential well depth, n_{ext} is the refractive index of the surrounding medium (water) and λ is the vacuum wavelength of interfering light waves.

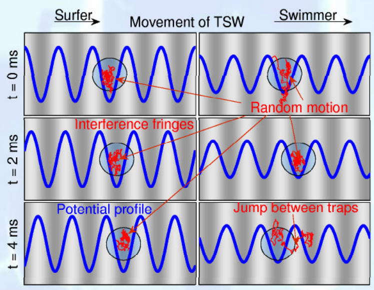

Figure 1. TSW moves with velocities 20 μms^{-1}, left column, and 40 μms^{-1}, right column. Trap depths are $\Delta U = 5\,k_BT$ in slower TSW and $\Delta U = 3.3\,k_BT$ in faster TSW. Interference fringes and potential profile are shown in 3 different times. The position of bead is symbolically shown by a blue circle and the random motion of bead between frames is shown by red line. The slower TSW demonstrates surfer case with bead still localized in one optical trap. The faster case shows swimmer case with jumps between neighboring optical traps.

Theoretical Results

To find out the mean velocity of particle in TSW it is necessary to find the time evolution of particle positions probability density $P(x,t)$. It is given by Fokker-Planck equation (FPE)

$$\frac{\partial}{\partial t}P(x,t) = \frac{\partial}{\partial x}\left\{\frac{U'(x)}{\eta}P(x,t)\right\} + \frac{k_BT}{\eta}\frac{\partial^2}{\partial x^2}P(x,t) \qquad (1)$$

and for the mean particle velocity one can obtain

$$\langle\dot{x}\rangle = v - \frac{Lk_BT}{\gamma}\frac{[\exp(\gamma vL/k_BT) - 1]}{\int_0^L \mathrm{d}x \int_x^{x+L} \mathrm{d}y \exp\left\{\frac{U(y)-U(x)+(y-x)\gamma v}{k_BT}\right\}}. \qquad (2)$$

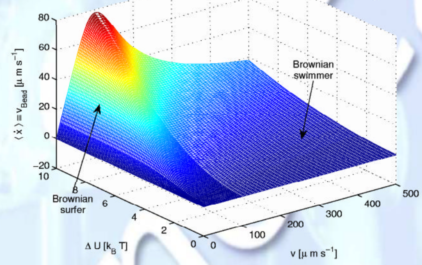

Figure 2. The mean velocity of a polystyrene bead of 520 nm in diameter placed to the traveling periodic potential. The limiting regions of the Brownian surfer(on the left) and the Brownian swimmer (on the right) are marked. The combinations of the wave velocity v and potential well depths ΔU can be found so that the particle velocity will be maximized.

Monte Carlo Simulation

Before the experimental realization, we used Monte Carlo (MC) simulations to study behavior of a bead in the TSW. In each simulation we performed at least 10^6 steps with a time lag between subsequent steps equal to 2.5 μs.

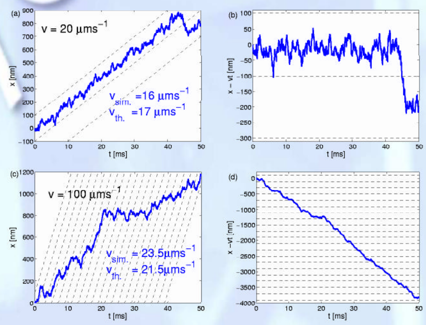

Figure 3. Monte-Carlo simulation of the bead positions in the traveling standing wave (TSW) with respect to the fixed coordinate system (a,c – left) and to the coordinate system traveling with standing wave (b,d – right). The following parameters were considered: trap depth $\Delta U = 5\,k_BT$ and bead diameter $d = 520$ nm. The dashed lines shows borders between neighboring optical traps. The speed of the TSW and the average velocity of the bead obtained from the MC simulation or Eq. (2) in this interval shown in (a, c).

Experimental Setup

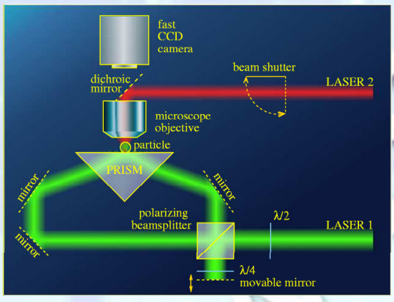

Figure 4. Schematic diagram of the experimental setup.

Results

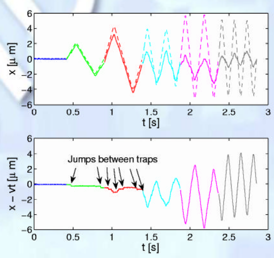

Figure 5 (←). Record of bead positions while TSW moves with different speeds. Left: positions of the bead during the movement (solid lines) and the displacement of the original bead position at $t = 0$ corresponding to the motion of the standing wave (dashed sawtooth curve). Right: the position of the bead with respect to TSW. Different colors show the different TSW speeds.

Figure 6 (↗). Histogram of bead positions from the part of record with TSW at rest. We used Boltzmann distribution to fit the trap depth ΔU.

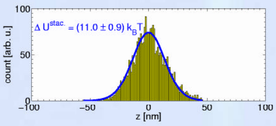

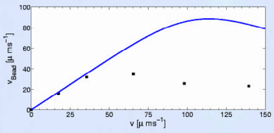

Processing the same data as shown in Fig. 5 we obtained the average speeds of the confined bead and also the speed of the TSW. We used histogram of bead positions in stationary TSW to find the trap depth $\Delta U = 11\,k_BT$, see Fig. 6. Using this ΔU we compared experimental data to the theoretical values from Eq. (2) without success as can be seen in Fig. 7. Therefore we assumed that the bead–surface distance changes as the bead starts to move. In case of stationary TSW the bead is in contact with surface while in motional TSW it moves up into the distance h. At this level the trap depth is lower since exponential decay of evanescent field an also the water viscosity changes, see Fig. 8. Experimental data were fitted by Eq. (2). The trap depth and viscosity were assumed as functions of bead–surface distance h and we found this separation. Figure 9 shows a good coincidence between fit and experimental data.

Note that the slowest TSW velocity provided optimal conditions for the existence of Brownian surfer. Faster TSW motion has not reached the conditions for Brownian swimmer and the bead was dragged by the TSW with smaller relative speed.

Figure 7 (↑). The experimentally obtained mean velocities of bead (squares) and the theoretical curve (blue line) obtained by Eq. (2). We used the trap depth $\Delta U = 11\,k_BT$ obtained from Fig. 6. There is no coincidence between experimental data and theoretical curve.

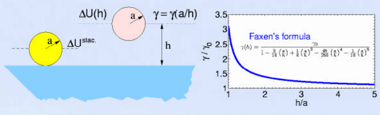

Figure 8 (↑). Left: The yellow bead is located in stationary TSW on the top of the prism while ping one is in the motional TSW in the distance h above prism. The rap depth in the h is $\Delta U(h) - \Delta U^{\text{stac.}}\exp(-\beta h)$; β is given by properties of incident wave. Right: the viscosity in h given by Faxen's formula.

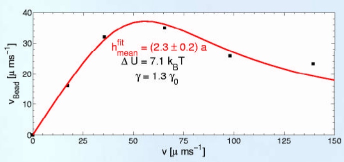

Figure 9 (←). The fit of experimental mean velocities of beads by Eq. (2). The trap depth and water viscosity were calculated as functions of mean bead–surface distance h, see Fig. 8. We obtained a good coincidence between experimental data and theory. The mean distance is (600 ± 50) nm and the values of trap depth and viscosity in this distance are shown in figure.

References

- H. Risken, *The Fokker-Planck Equation*, Springer-Verlag, Berlin, 1996.
- P. Reimann, "Brownian motors: noisy transport far from equilibrium," *Physics Reports* **361**, pp. 57–265, 2002.
- M. Šiler, T. Čižmár, M. Šerý, and P. Zemánek, "Optical forces generated by evanescent standing waves and their usage for sub-micron particle delivery," *Appl. Phys. B* **84**, pp. 157–165, 2006.
- T. Čižmár, M. Šiler, M. Šerý, P. Zemánek, V. Garcés-Chávez, and K. Dholakia, "Optical sorting and detection of sub-micron objects in a motional standing wave," *Phys. Rev. B* **74**, pp. 035105, 2006.

Acknowledgments

This work was partially supported by the Institutional Research Plan of the Institute of Scientific Instruments (AV0Z20650511), Grant Agency of the Academy of Sciences (IAA1065203), European Commission via 6FP NEST ADVENTURE Activity (ATOM3D, project No. 508952), and Ministry of Education, Youth, and Sports of the Czech Republic (project No. LC06007).